Compact beam expander with linear gratings

Revital Shechter, Yaakov Amitai, and Asher A. Friesem

Novel compact beam expanders that could be useful for applications such as providing light to flat panel displays are presented. They are based on a planar configuration in which three spatially linear gratings are recorded on one transparent substrate, so as to expand a narrow incoming beam in two dimensions. We present the design and recording procedures along with results, showing a relatively uniform intensity of the wide output beam. Such expanders can serve for illuminating flat panel displays. © 2002 Optical Society of America

OCIS codes: 050.1970, 050.1950, 090.2890.

1. Introduction

Beam expanders for magnifying a narrow collimated beam into a beam of larger diameter typically comprise a telescopic assembly of two refractive lenses or mirrors along a common axis with a common focal point. They have been implemented in a variety of applications, such as lasers,[1–3] fibers,[4] medical diagnostics,[5] holography,[6–8] x-ray optics,[9] and space and atmospheric research.[10,11] When using monochromatic light, it may be advantageous to replace the refractive lenses with separated diffractive optical elements (DOEs) with the optical power[12] to form compact configurations.[13–15] DOEs are difficult to exploit fully because of their excessive aberrations and because turning to polychromatic light causes chromatic dispersion.

Here we present a method for designing and recording a compact beam expander that comprises DOEs that are relatively simple linear gratings, all recorded in a planar configuration on one substrate. The beam expander expands an incoming beam by means of splitting and combining operations, with no need for optical power from the expanding elements. This makes the beam expander more robust and allows it to be used with both monochromatic as well as polychromatic light. Typically, the planar beam expander comprises two or three DOEs for expanding in one or two dimensions, respectively. The first couples the light into the substrate. The second expands it in one dimension and directs it to the third DOE, if such exists. The final DOE, second or third, couples the expanded light out of the substrate to yield a large, uniform, beam light. To ensure that the output beam will have a uniform light intensity distribution, the diffraction efficiency at each point must differ. We developed design and recording procedures to control the diffraction efficiency at each point and obtain uniform light distribution at the output. Initially, we designed, recorded, and evaluated a planar configuration that expands an incoming beam in one dimension only and then a configuration that expands an incoming beam in two dimensions.

2. Beam-Expanding Configurations

We begin with the simple planar configuration, shown in Fig. 1, in which a narrow beam is expanded in one dimension. It comprises a pair of DOEs, both recorded on one substrate. The first DOE is a small linear grating that couples the light into the substrate, whereas the second DOE is a larger linear grating recorded to have varying diffraction efficiency, so that light impinging several times on it will emerge with the same intensity at each exit point.

We then calculate the required diffraction efficiency at each output point on the second DOE to achieve uniform intensity at the output. We denote the diffraction efficiency at the first output point μ_1. We require that the intensity of the output beam at all output points be identical. The intensity of the output beam at the mth output lateral point can be written as $T_m = \mu_m \times I_m$, where μ_m is the diffraction efficiency at this point and I_m is the intensity inside the substrate that impinges on this point. We then compared two consecutive output beams to obtain the

The authors are with the Department of Physics of Complex Systems, Weizmann Institute of Science, 76100 Rehovot, Israel. R. Shechter's e-mail address is ferevita@wisemail.weizmann.ac.il.

Received 5 April 2001; revised manuscript received 16 August 2001.

0003-6935/02/071236-05$15.00/0

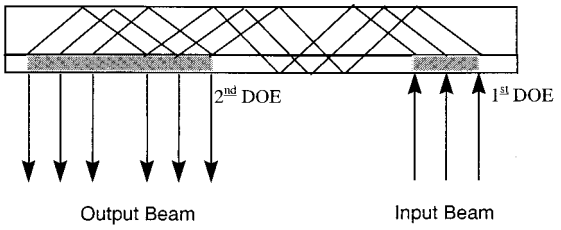

Fig. 1. Planar configuration of a beam expander in one dimension.

following equation for μ_m at the mth output lateral point,

$$\mu_m = \frac{\mu_1}{1 - (m - 1)(1 + \alpha)\mu_1}, \tag{1}$$

where α is the loss, if any, inside the substrate. The results, assuming no losses ($\alpha = 0$) and taking the diffraction efficiency at the last output point, here the fifth output, to be 100%, in order to utilize all the light, are presented in Fig. 2. As shown, the diffraction efficiency behaves as an increasing geometrical function along the lateral coordinate of the DOE.

The planar configuration for expanding a narrow beam of light in two dimensions is shown in Fig. 3. Figure 3(a) is a top view. Figure 3(b) is a side view. It comprises three laterally displaced DOEs that are recorded on a single substrate. The first DOE H_1 collimates the incident light from the source (if the light is not collimated already) and diffracts the input incident light into the substrate, so it will propagate toward the second DOE H_2, by total internal reflection.

Assuming that the input beam is normally incident onto H_1, the diffraction angle inside the substrate is β, and the propagation direction of the diffracted beam inside the substrate is along the ξ axis, then the grating function of H_1 is

$$\Phi_1 = -\frac{2\pi}{\lambda}(v \sin \beta)\xi, \tag{2}$$

where v is the refractive index of the substrate and λ is the wavelength, in air, of the incident light. DOE H_1 should have a uniformly high diffraction efficiency so that most of the input incident light is coupled into the substrate.

After several reflections inside the substrate, the

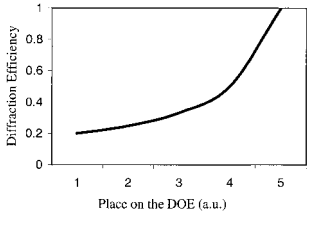

Fig. 2. Required diffraction efficiency as a function of lateral spatial coordinate on the second DOE; a.u., arbitrary units.

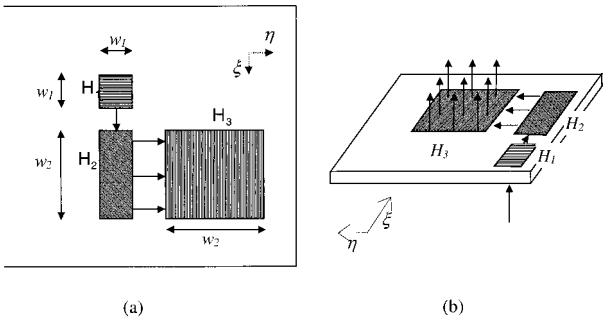

Fig. 3. Top view of the planar configuration for expanding a narrow beam in two dimensions.

diffracted beam from H_1 reaches the second DOE H_2, where it is redirected toward the third DOE H_3. The characteristics of H_3 are that along the axis η, which is normal to the propagation axis ξ, the lateral dimension of H_1 is w_1; and along the axis ξ the lateral dimension w_2 is substantially larger than w_1, depending on the desired expansion along that direction, i.e., w_2/w_1. The size of w_1 is determined by the lateral length of one round trip of the beam inside the substrate. This is done to insure that no overlap will occur between beams of two adjacent output points. Therefore, w_1 will depend on the thickness of the substrate, the central propagation angle β inside the substrate, and the field of view. The local diffraction efficiency of H_2 is not a constant but increases gradually along the ξ axis. Specifically, DOE H_2 must be recorded so that its localized diffraction efficiency will increase nonlinearly with distance along the ξ axis, to obtain a uniform output-beam light distribution, as shown in Fig. 4.

We require now that the central beam diffracted from H_2 will still be oriented at the angle β but will propagate along the η axis, making a 90° bend inside the substrate. Hence, the grating function of H_2 has to cancel out the phase function Φ_1 from Eq. (2) and

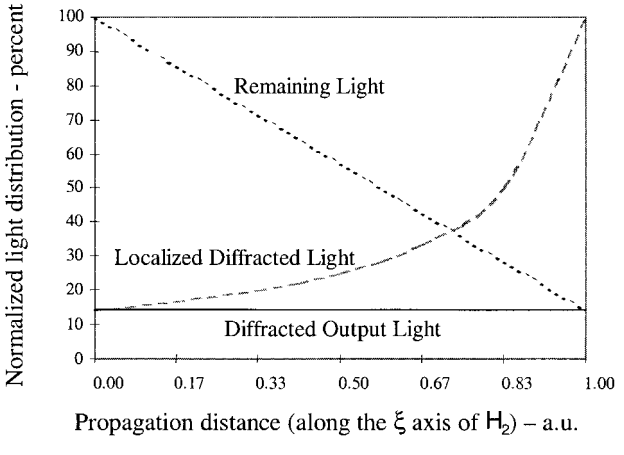

Fig. 4. Light distribution as a function of the distance along the ξ axis of H_2. a.u., arbitrary units.

leave an identical phase term in the μ direction. This can be written as

$$\begin{aligned}\Phi_2 &= -\Phi_1 + \frac{2\pi}{\lambda}(v \sin\beta)\eta \\ &= \frac{2\pi}{\lambda}(v \sin\beta\xi + v \sin\beta\eta) \\ &= \ldots \frac{2\pi}{\lambda}\frac{\sqrt{2}}{2} v \sin\beta\left(\frac{\sqrt{2}}{2}\xi + \frac{\sqrt{2}}{2}\eta\right) \\ &\quad + \frac{2\pi}{\lambda}\frac{\sqrt{2}}{2} v \sin\beta\left(\frac{\sqrt{2}}{2}\xi + \frac{\sqrt{2}}{2}\eta\right). \qquad (3)\end{aligned}$$

The grating function of Eq. (3) can be achieved by recording the pattern resulting from the interference of two plane waves that are oriented at angles of $\pm\beta'$ with respect to the normal to the recording medium, where $\sin\beta' = \sqrt{2}/2 \sin\beta$ and the projection of the recording plane waves on the substrate is along the bisector of the angle between ξ and η.

The optical beam, diffracted from H_2, is trapped in the substrate and propagates toward the third DOE H_3, where it is diffracted in a normal direction, out of the substrate. This DOE H_3 has dimensions of w_2 in both lateral directions, and its localized diffraction efficiency also increases gradually, as for H_2, but only along the η axis.

The grating function of DOE H_3 is

$$\Phi_3 = -\frac{2\pi}{\lambda}(v \sin\beta)\eta. \qquad (4)$$

Similarly to H_2, DOE H_3 also expands the size of the incoming beams by a factor of w_2/w_1—but along the η axis. Thus the combination of the three DOEs increases the size of the incident input beams by a factor of w_2/w_1 in both axes.

Combining Eqs. (2)–(4) yields

$$\Phi_1 + \Phi_2 + \Phi_3 = 0. \qquad (5)$$

Which means that the total configuration does not add phase, other than multiple integers of λ, to an incoming beam. Equation (5) is valid for all wavelengths, so the overall planar configuration will have no chromatic dispersion and is therefore appropriate for polychromatic light. Typically the output beam emerges in the same direction as the incoming beam. But, it is also possible to record DOE H_3, so the output beam will emerge in a direction opposite that of the incoming beam.

3. Experimental Procedures and Results

To obtain the required varying local diffraction efficiency in the second and third DOEs, we varied the local exposure by letting the light of the recording beams pass through a varying neutral-density mask. The mask was either a silver halide film with varying gray levels or a glass plate on which copper was deposited with locally varying layer thickness.

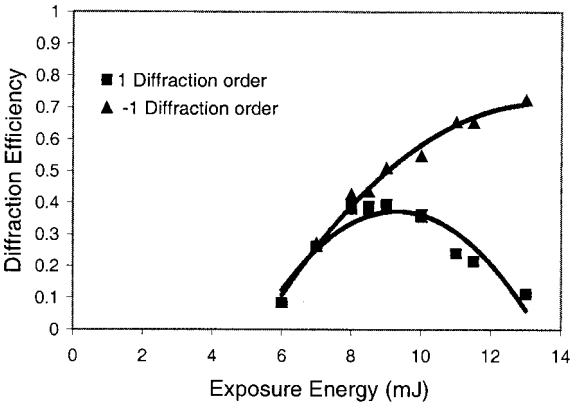

Fig. 5. Diffraction efficiency as a function of exposure energy for Shipley's 1805 photoresist.

To fabricate the copper mask, we measured the transmission of thin layers of copper on glass at a 363.8-nm wavelength. We then measured the dependence of diffraction efficiency of the recording material, Shipley's 1805 photoresist, on exposure energy. The recording wavelength was 363.8 nm, and the readout wavelength was 514.5 nm. Figure 5 presents results of one set of measurements. The results show that the diffraction efficiency can be controlled from zero to about 80% efficiency in the desired order.

The results of the copper transmission measurements and of Fig. 5 were then used to calibrate diffraction efficiency as a function of copper thickness. We then used our calculated desired diffraction efficiency (Fig. 2) to coat a mask on glass with the desired varying thickness of the copper layer. To fabricate the silver halide mask, we measured the transmission of the silver halide emulsion as a function of the gray level. The results of these measurements and of Fig. 5 were then used to calibrate diffraction efficiency as a function of gray level. We then used the masks to record the planar configuration and evaluated its performance. The recording of a DOE through a mask is shown in Fig. 6.

Figure 7 shows experimental results of output-beam intensity as a function of lateral location on a second grating for two grating pairs. One is a grating pair for which the second, extended grating, was recorded with locally varying diffraction efficiency. The second was a standard grating pair, for which both gratings were recorded with uniform diffraction efficiency. It is evident that the variation in diffrac-

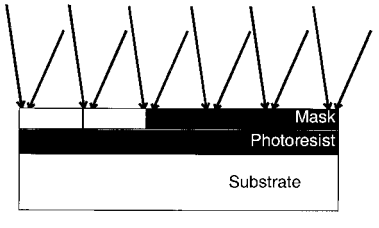

Fig. 6. Recording through a locally varying mask.

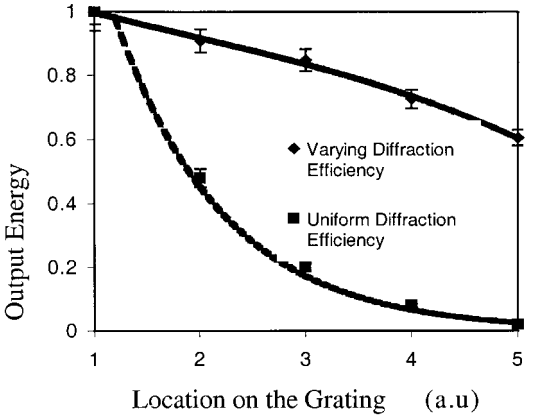

Fig. 7. Output light intensity as a function of location on the second grating. a.u., arbitrary units.

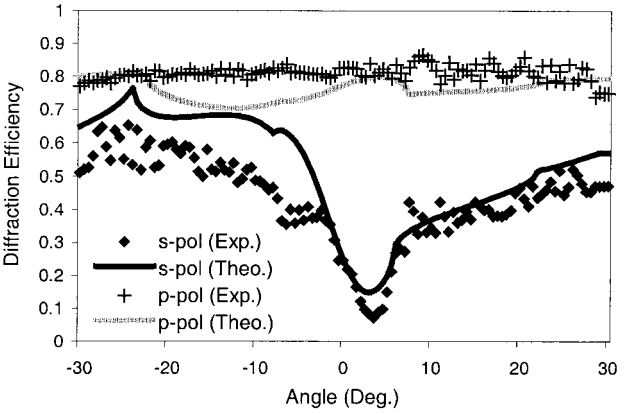

Fig. 9. Diffraction efficiency of the zero order as a function of angle.

tion efficiency improves the uniformity of the output intensity. The uniformity is not yet perfect, mainly because of imperfections in the recording and mask fabrication procedures.

We recorded the first DOE with constant diffraction efficiency for all our samples. The second and third DOEs were recorded either with constant diffraction efficiency or with varying diffraction efficiency, using silver halide or copper masks, according to the procedure described above. The triple-element configuration was then evaluated. First, we illuminated each of the elements with white light and recorded its spectral response. Figure 8 shows representative results of such a scan, done in both polarizations, along with the results of theoretical calculations. Because of instrument limitations we could scan directly only the zero order of the gratings. The desired first-order efficiency can be calculated with the aid of Fig. 5. As a general rule, decreasing the efficiency of the zero order increases the efficiency of the first order. The theoretical calculations were based on the parameters of recording and atomic-force microscope scans to retrieve depth and shape of the gratings. Generally, the experimental results fit the shape of the theoretical results. The difference can be explained by fabrication errors, which are not taken into account, and errors in the data taken from the atomic-force microscope scans. Figure 8 reveals that both polarizations have better efficiency for the first order in the shorter wavelengths of the visible spectrum. The *p* polarization has lower first-order efficiency than that of the *s* polarization. The *s* polarization has an additional peak of efficiency near the designed wavelength of 514.5 nm. Overall, Fig. 8 shows that although the configuration can be used with polychromatic light, care should be taken, with a special filter, to cancel out the chromatic response of the gratings.

We then evaluated our gratings by scanning the output as a function of incidence angle. Figure 9 shows representative results of these scans. Again they were done in both polarizations. In these scans too the experimental results fit the shape of the theoretical results, where the difference can be explained by the same error factors as in Fig. 8. Figure 9 reveals that the *p* polarization has a practically constant, but low, first-order efficiency over

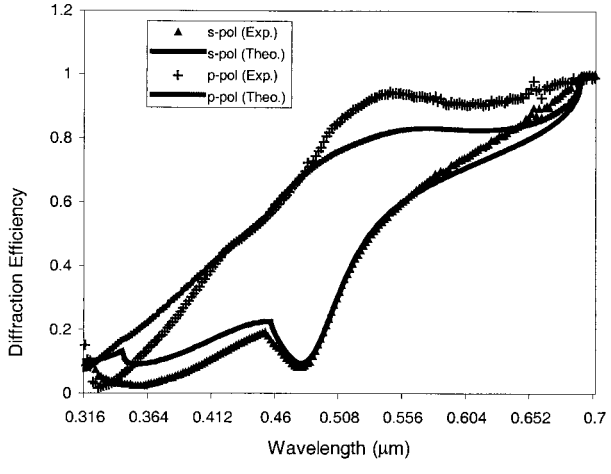

Fig. 8. Diffraction efficiency of the zero order as a function of wavelength.

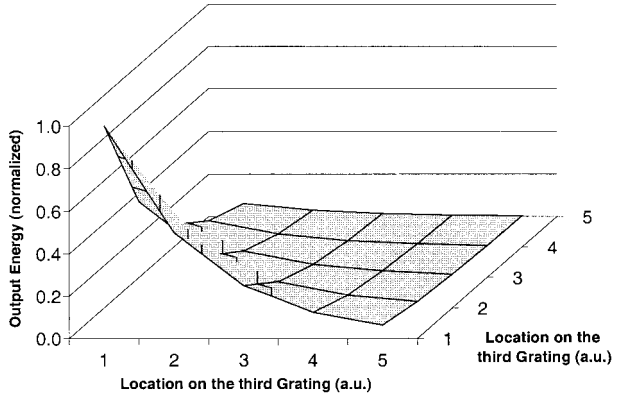

Fig. 10. Output light intensity as a function of location on the third grating for constant diffraction efficiency; a.u., arbitrary units.

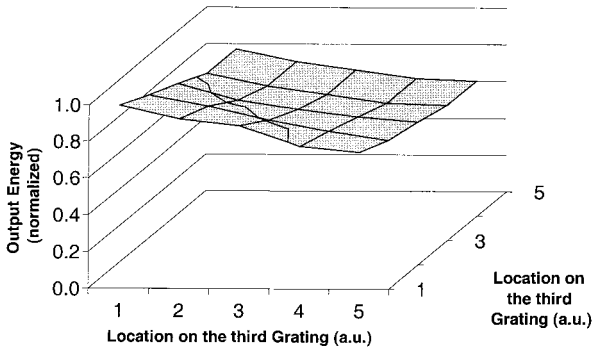

Fig. 11. Output light intensity as a function of location on the third grating for varying diffraction efficiency; a.u., arbitrary units.

the entire field of view. The *s*-polarization beam has very good first-order efficiency in a region of a few degrees near the designed zero incidence angle and good efficiency over a larger region between −20 and 20 deg. We can see that the response to the incidence angle needs to be improved, which we intend to do in further study in the near future.

Then we illuminated the first DOE with green light (514.5 nm) and looked at the output of the third DOE with constant or varying diffraction efficiency. The results shown in Fig. 10 are for a configuration with constant diffraction efficiency. As expected the intensity at the output is highly nonuniform and drops rapidly away from the first output point. Figure 11 shows the output of a configuration with varying diffraction efficiency. Evidently, the results show that even for a three-element configuration we can obtain a fairly uniform output beam.

In addition we illuminated a three-gratings configuration, where the second and third gratings were recorded with varying diffraction efficiency according to our design procedures, with a narrow input beam of 1–2 mm. We then took pictures of the multiple output points of the beam from the third grating. One typical picture is shown in Fig. 12. The points are uniform in intensity and of the same shape.

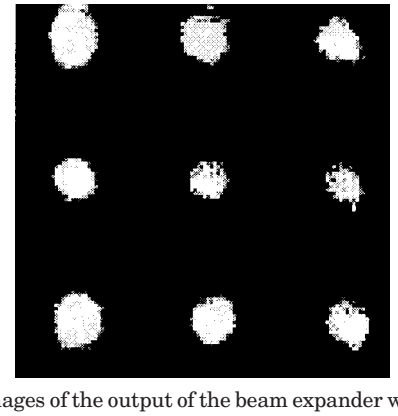

Fig. 12. Images of the output of the beam expander with a narrow input.

4. Concluding Remarks

We have presented a design and recording configurations for compact beam expanders that are useful with monochromatic as well as polychromatic light. They are made up of simple linear diffraction gratings. A beam expander in which a narrow beam was magnified by a factor of 25 (5 in each dimension) was experimentally evaluated. The results revealed that the light distribution could be practically uniform over the entire output area. In the future we intend to address the issues of angular and spectral response of the beam expander.

References

1. M. Chapman and N. R. Heckenberg, "Use of a beam expanding telescope in grating-tuned waveguide CO_2 laser," Int. J. Infrared Millim. Waves **8,** 783–791 (1987).
2. M. Bea, A. Giesen, M. Huonker, and H. Hugel, "Flexible beam expanders with adaptive optics—a challenge for modern beam delivery," in *Beam Control, Diagnostics, Standards, and Propagation*, L. W. Austin, A. Giesen, D. H. Leslie, and H. Weichel, eds., Proc. SPIE **2375,** 84–95 (1995).
3. M. Takahashi and T. Ohntoshi, "Finite-difference time-domain analysis of laser diodes integrated with tapered beam-expanders," IEEE Photon Tech. Lett. **11,** 524–526 (1999).
4. F. Martinez, G. Wylangowski, C. D. Hussy, and F. P. Payne, "Practical single-mode fibre-horn beam expander," Electron. Lett. **24,** 14–16 (1988).
5. S. K. Gayen, M. E. Zevallos, B. B. Das, and R. R. Alfano, "Time-sliced, two-dimensional, near-infrared imaging of normal and malignant human breast tissues," *Conference on Lasers and Electro-Optics* (*CLEO/U.S.*), Vol. 6 of 1998 OSA Technical Digest Series (Optical Society of America, Washington, D.C., 1998), pp. 230–231 (1998).
6. P. Hariharan, "Beam expander for making large rainbow holograms," Appl. Opt. **26,** 1815–1818 (1987).
7. Wu Jiang, D. L. Shealy, and K. M. Baker, "Physical optics analysis of the performance of a holographic projection system," in *Diffractive and Holographic Optics Technology*, I. Cindrich and S. H. Lee, eds., Proc. SPIE **2404,** 227–234 (1995).
8. S. B. Odinokov and M. V. Borisov, "Optical system of the device for making a hologram matrix," in *Diffraction and Holographic Technologies, Systems, and Spatial Light Modulators*, I. Cindrich, S. H. Lee, and R. L. Sutherland, eds., Proc. SPIE **3633,** 279–284 (1999).
9. F. E. Christensen, A. Horntrup, P. Frederiksen, C. Nilsson, P. Grundsoe, P. Orup, E. Jacobsen, H. W. Schnopper, R. Lewis, and C. Hall, "A beam expander facility for studying x-ray optics," Rev. Sci. Instrum. **63,** 1168–1171 (1992).
10. M. S. Scholl and G. N. Lawrence, "Diffraction modeling of a space relay experiment," Opt. Eng. **29,** 271–278 (1990).
11. R. Neubert, L. Grunwaldt, G. Sesselmann, and M. Steinbach, "An innovative telescope system for SLR," in *Laser Radar Ranging and Atmospheric Lidar Techniques II* (*Europto*), U. Schreiber and C. Werner, eds., Proc. SPIE **3865,** 83–89 (1999).
12. V. Neuman, C. W. Pitt, and L. M. Walpita, "Guided-wave holographic grating beam expander—fabrication and performance," Electron. Lett. **17,** 165–167 (1981).
13. R. K. Kustuk, M. Kato, and Y. T. Huang, "Substrate mode holograms for optical interconnects," in *Optical Computing*, Vol. 9 of 1989 OSA Technical Digest Series (Optical Society of America, Washington, D.C., 1989), pp. 168–171.
14. A. A. Friesem and Y. Amitai, "Planar diffractive elements for compact optics," in A. Consortini, ed., *Trends in Optics* (Academic, San Diego, 1996), pp. 125–144.
15. I. Shariv, Y. Amitai, and A. A. Friesem, "Compact holographic beam expander," Opt. Lett. **18,** 1268–1270 (1993).